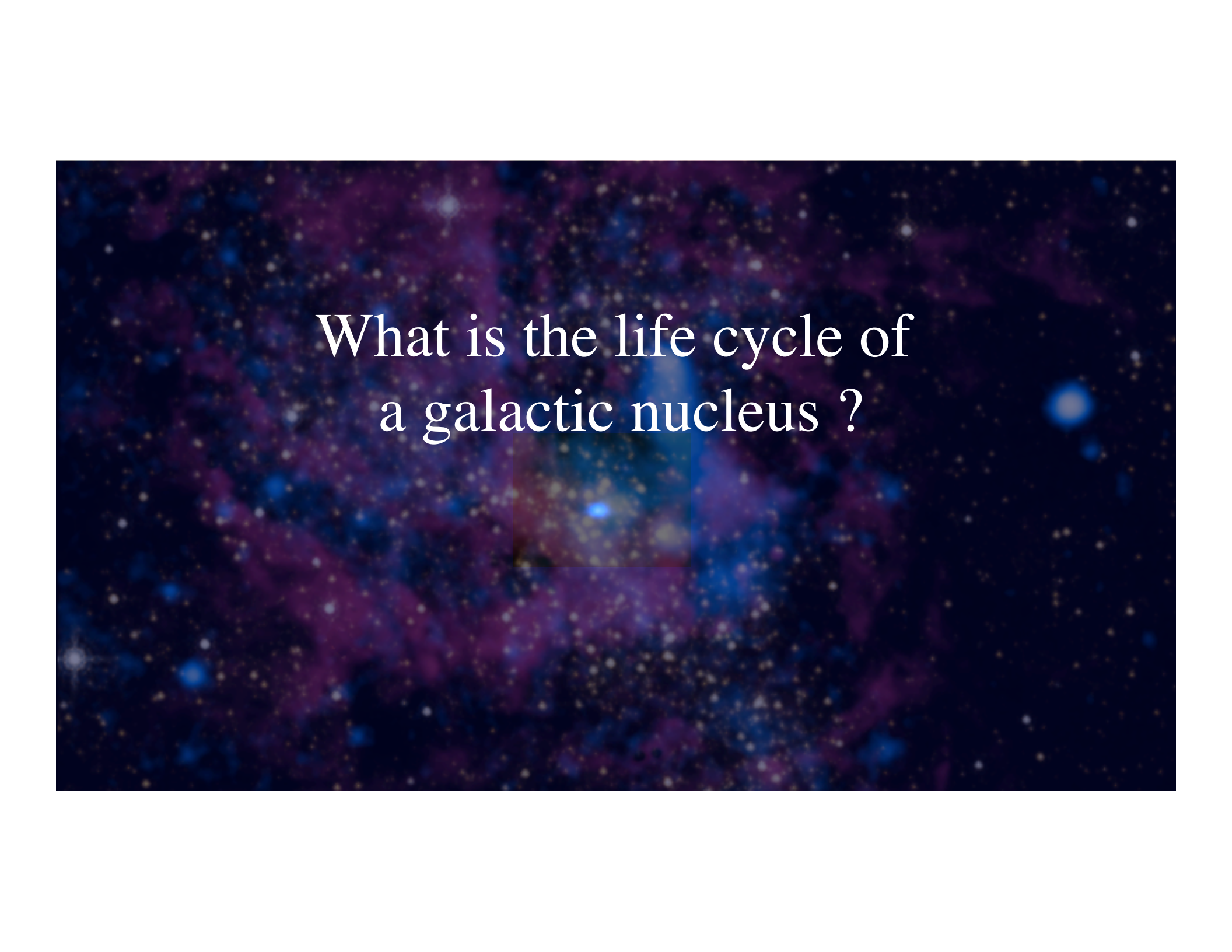




Flows and Flares around the Nearest Massive Black Hole -- Sgr A*

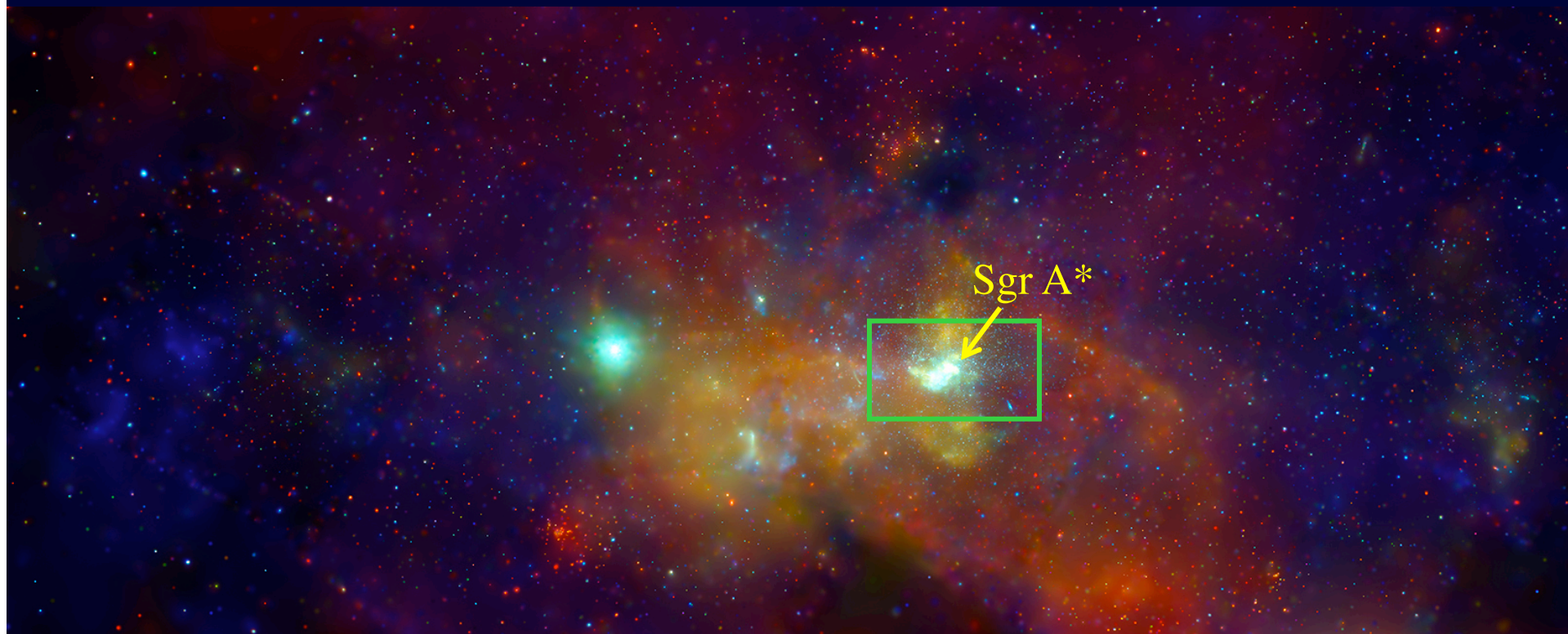
Q. Daniel Wang

University of Massachusetts



What is the life cycle of
a galactic nucleus ?

The Galactic center as viewed by Chandra



Red: 1-2.5 keV Green: 2.5-4 keV Blue: 4-9 keV

Wang et al. 02

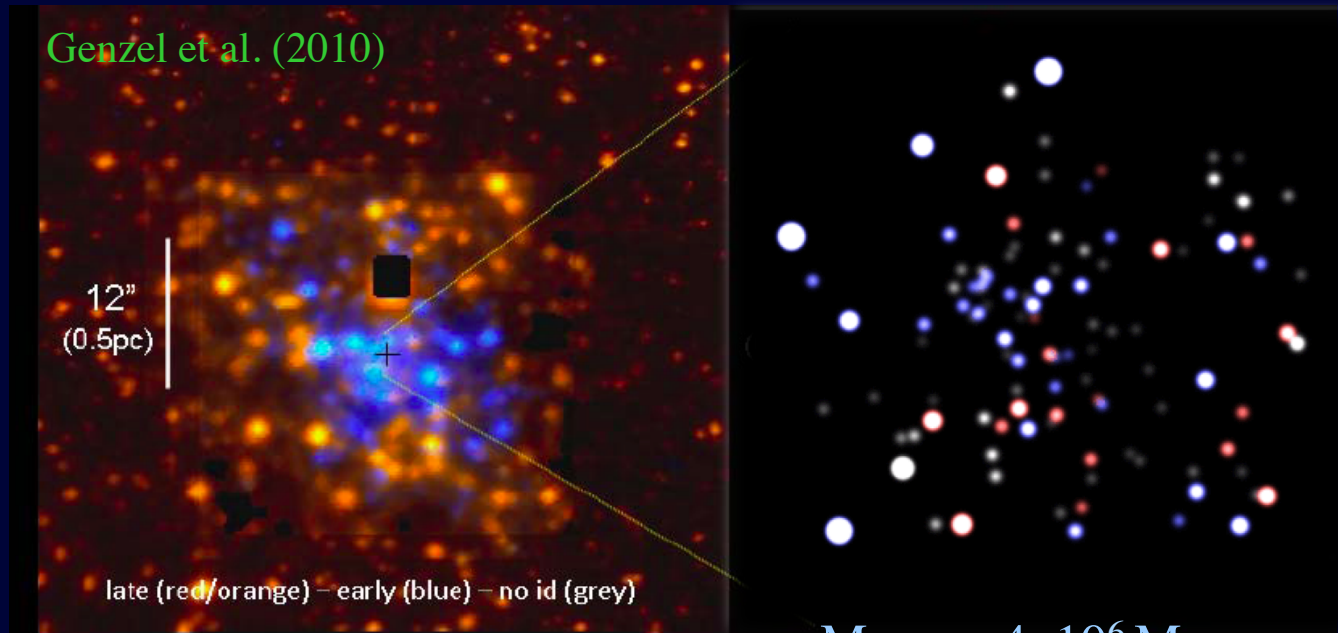
The Galactic center in NIR



Mini-spiral
representing the ionized part of the CND

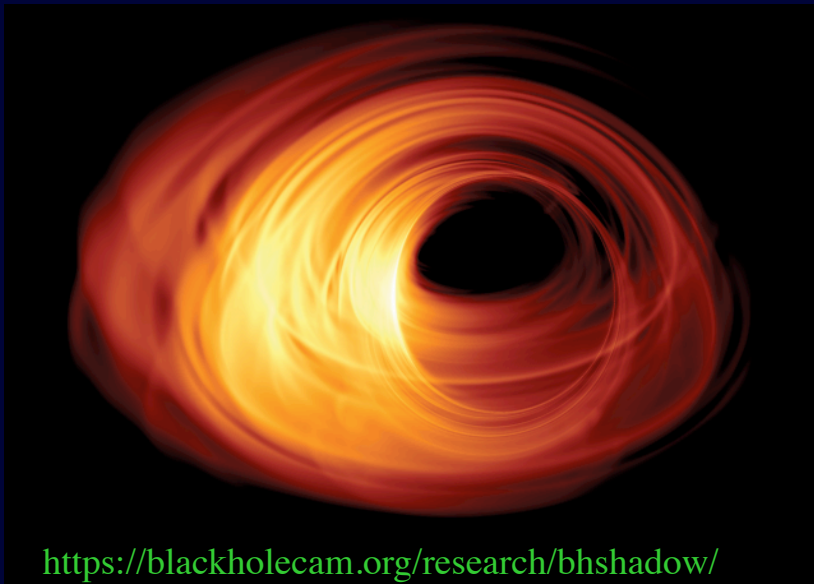
HST/NICMOS $P\alpha$ + continuum map (Wang et al. 10)

The Galactic center in NIR

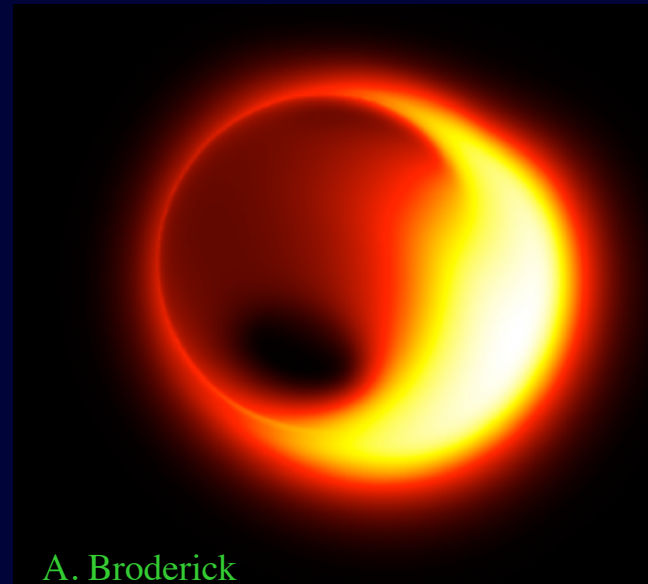


- Central cluster: ~ 100 O & WR stars, many in a disk
- Colliding stellar winds $\rightarrow 10^7$ K gas
- $M_{\text{MBH}} = 4 \times 10^6 M_{\odot}$
- $L_x = 3 \times 10^{33}$ erg/s
- $L_{\text{bol}} = \text{a few } \times 10^{36} \text{ erg/s or } \sim 10^{-8} L_E$ -- peaking in submm!

What you wish to see Sgr A* at (sub)mm



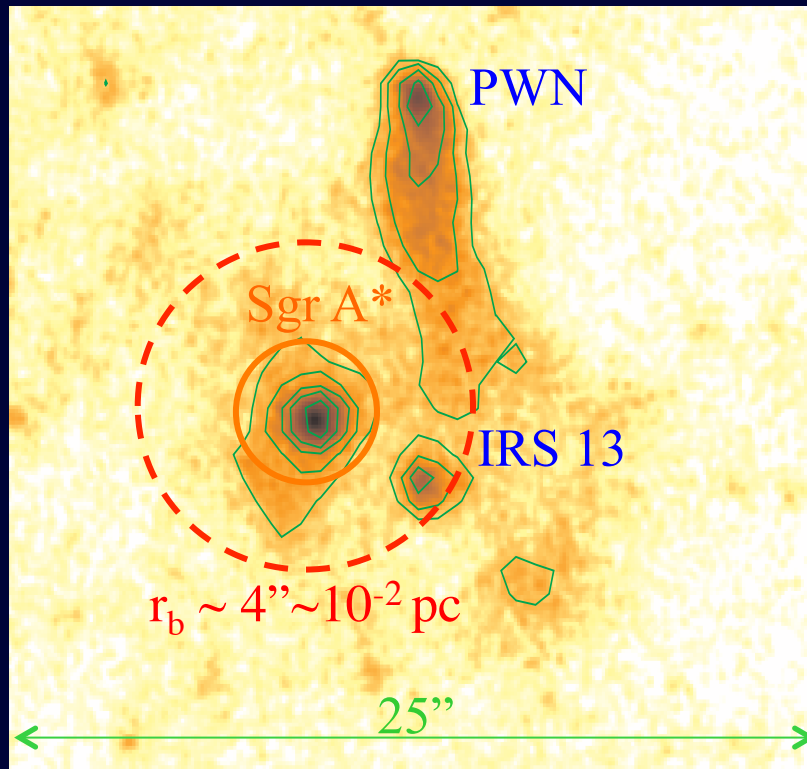
<https://blackholecam.org/research/bhshadow/>



A. Broderick

- (sub)mm emission arises in the innermost region ($r < 10^2 r_s$)
- Its morphology depends on as the spin of the MBH, as well the accretion and emission models.

Sgr A* in X-ray



1-9 keV image from 3 Ms Chandra XVP (2012)

Hot gas accretion rate

$$\dot{M}_b \sim 2 \times 10^{-5} M_{\odot}/\text{yr} (M_{\text{MBH}}/4 \times 10^6 M_{\odot})^2 (n_e/10^2 \text{ cm}^{-2})(T/10^7 \text{ K})^{-3/2}$$

$\Rightarrow L_b \sim 2 \times 10^{41} \text{ erg/s}$ (assuming a 10% radiative efficiency) or $\sim 10^5$ greater than L_{bol} of Sgr A*.

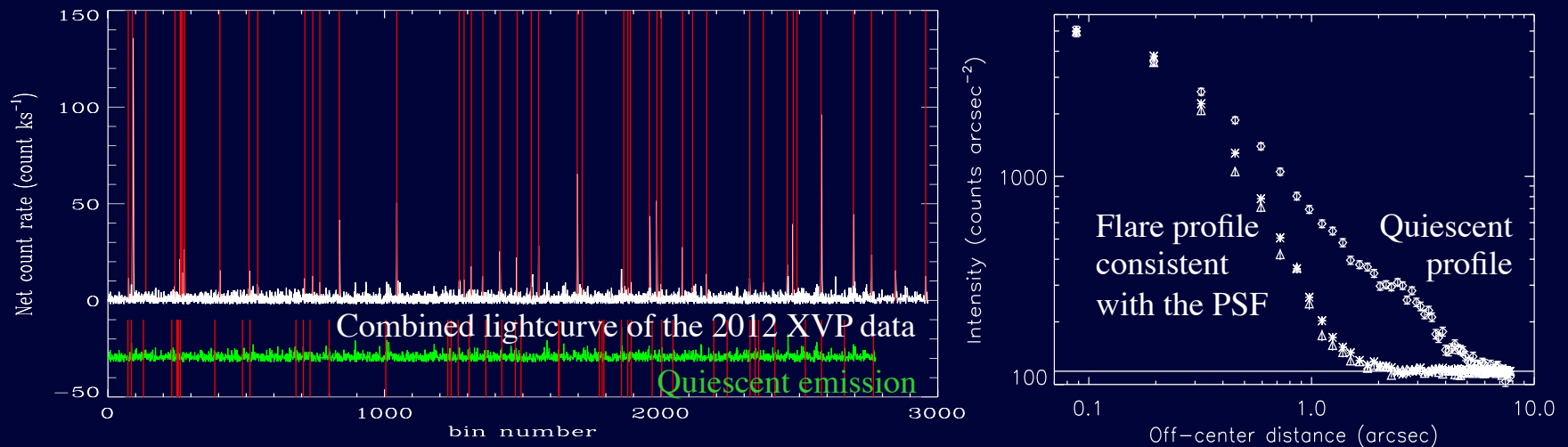
So it is a radiatively inefficient accretion flow (RIAF)!

Where does the energy go? Or is there much of accretion at all?

Wang et al. 13

Dissecting X-ray emission of Sgr A*

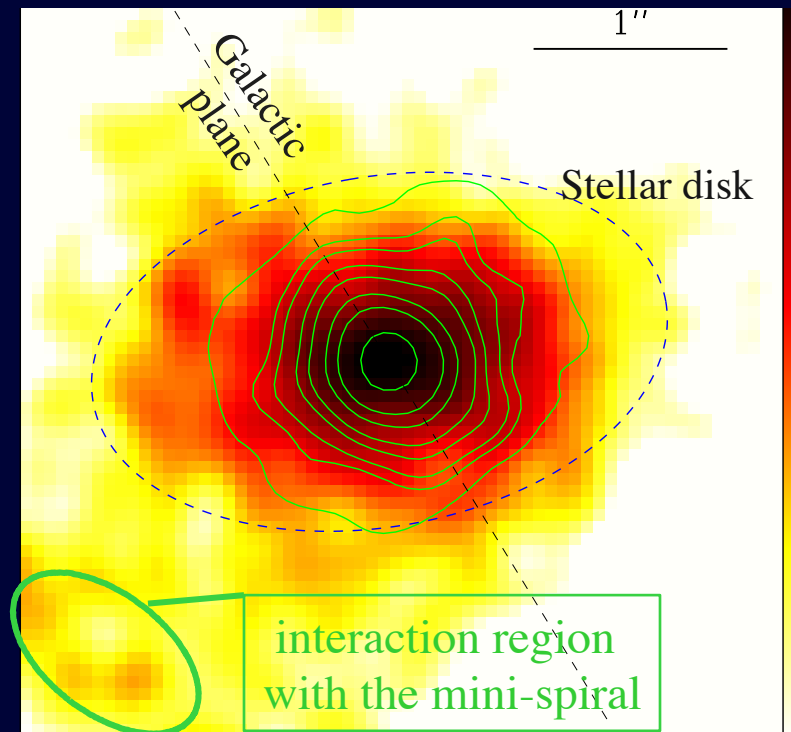
Decompose flare and quiescent components



- Detected flares account for $\sim 1/3$ of the total X-ray flux.
- Flare emission is point-like.
- Quiescent emission is extended on 4'' scales.

Wang et al. 13; Neilsen et al. 13; Yuan & Wang 16

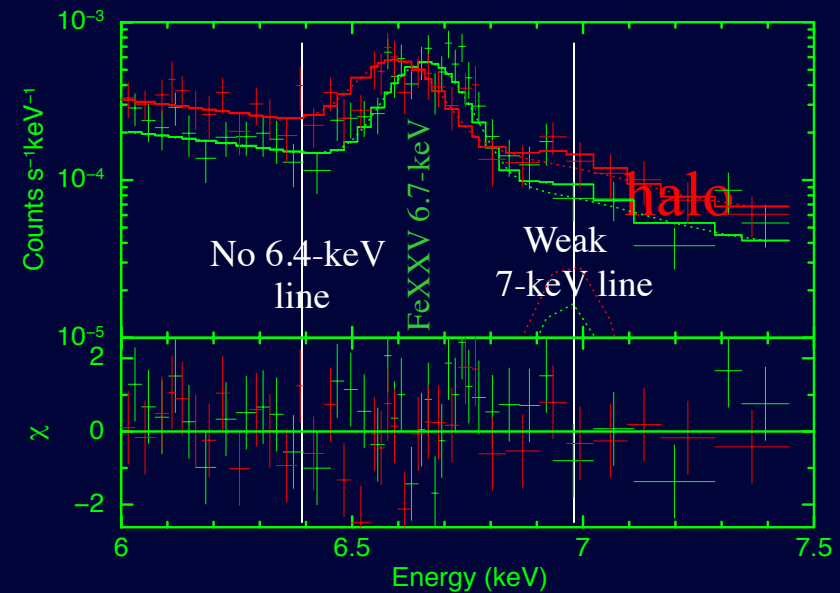
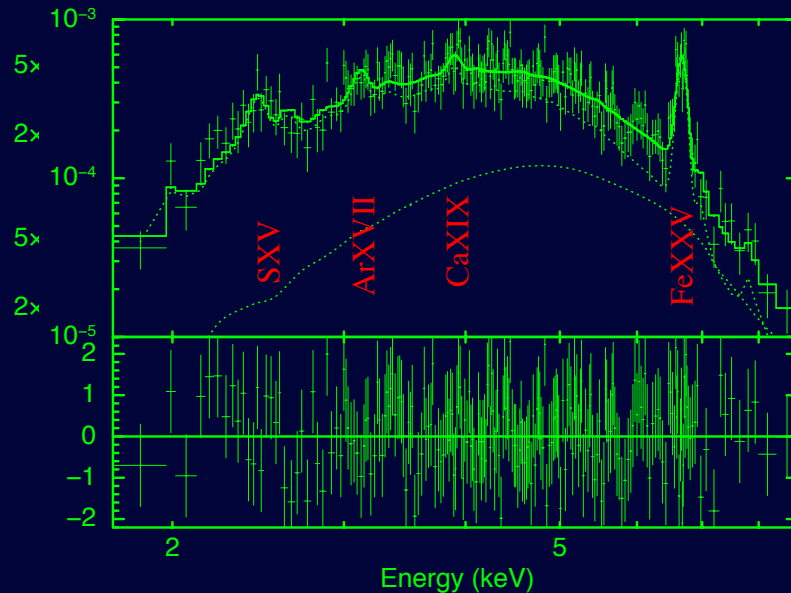
Model the quiescent X-ray emission



- Residual point-like component $< 20\%$ of the flux within $1.5''$ radius.
- Elongation of the extended component is consistent with the orientation of the stellar disk.
- Apparent enhancement due to the wind interaction with the mini-spiral of cool gas.

Wang et al. (2013)

X-ray spectral testing of RIAF solutions



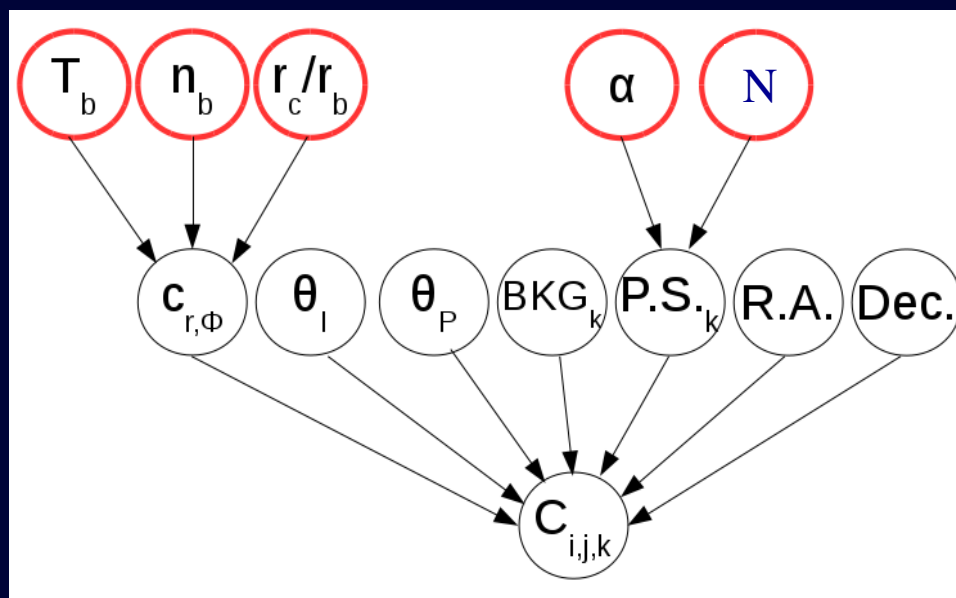
- ADAF solution without mass-loss \rightarrow inconsistent large FeXXVI/FeXXV $K\alpha$ ratio, too flat continuum, & too low metal abundance.
- Best-fit model requires mass-loss $> 99\%$ -- the prediction of the adiabatic inflow-outflow solution (e.g., Blandford & Begelman 04).

Summary: 1-D X-ray dissection results

- No indication for any cold accretion!
- Bulk of the quiescent X-ray emission is **optically-thin thermal** and arises from **outer regions** ($r \sim 10^4\text{-}10^5 r_s$) of the accretion flow.
- Contrast to AGN, in which innermost regions dominate.
- **Outflow nearly balances the inflow.**
- Why should the outflow occur?
- What is the origin of the central point-like source?

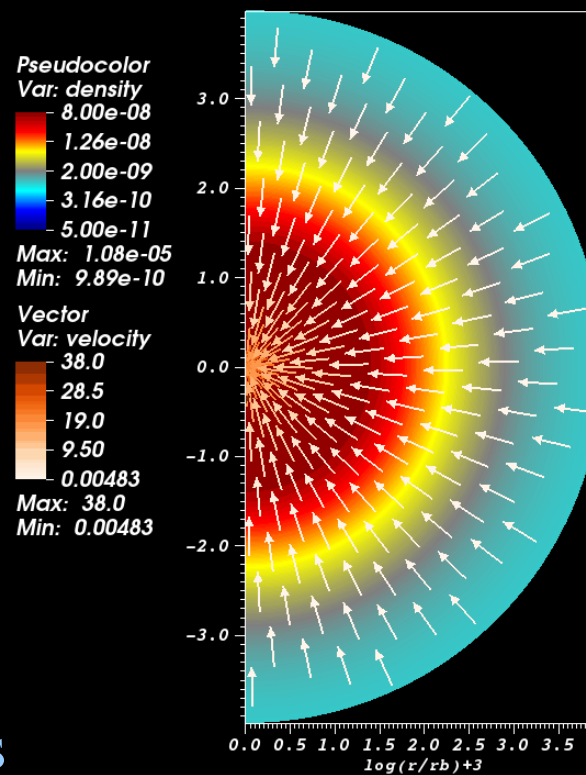
Toward physical modeling
of the accretion and outflow

Simulations and Bayesian fit



- Projection
 - PSF convolution
- ⇒ count images in three bands

Roberts, Jiang, QDW, & Ostriker 17



Time/0.1Tb=0

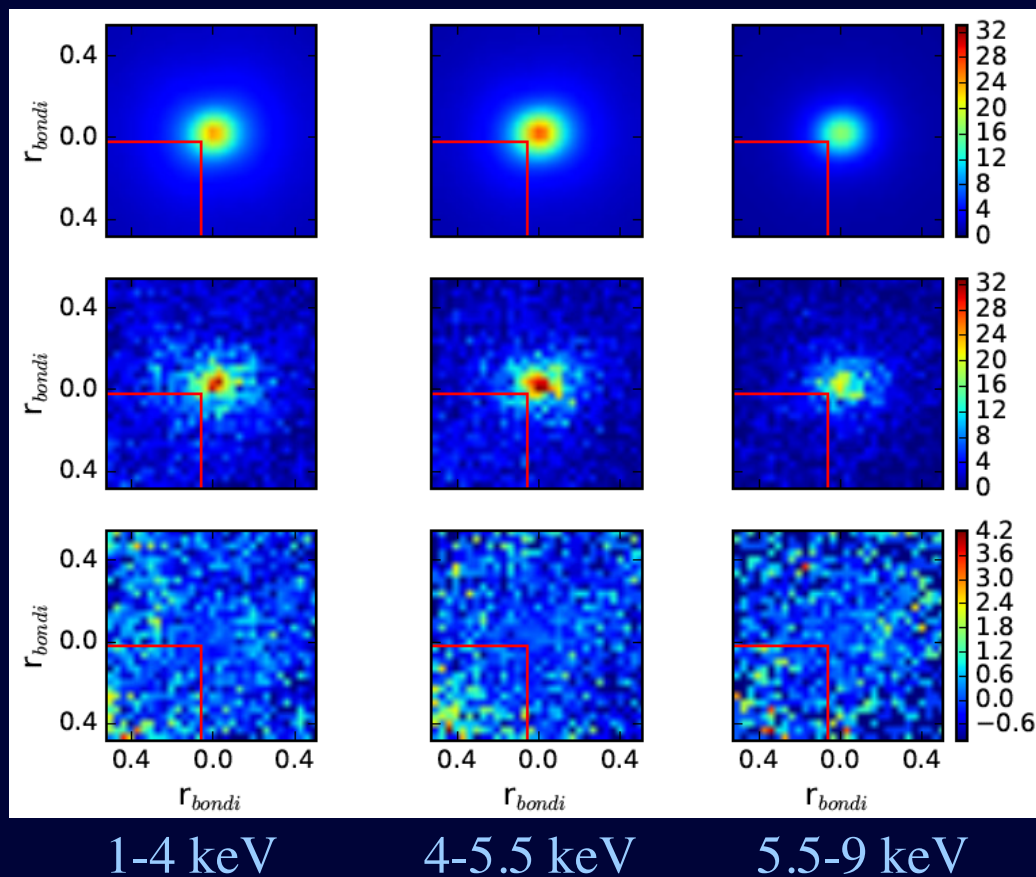
user: YanFei
Tue Apr 22 12:29:07 2014

Best-fit model compared with data

Model

Data

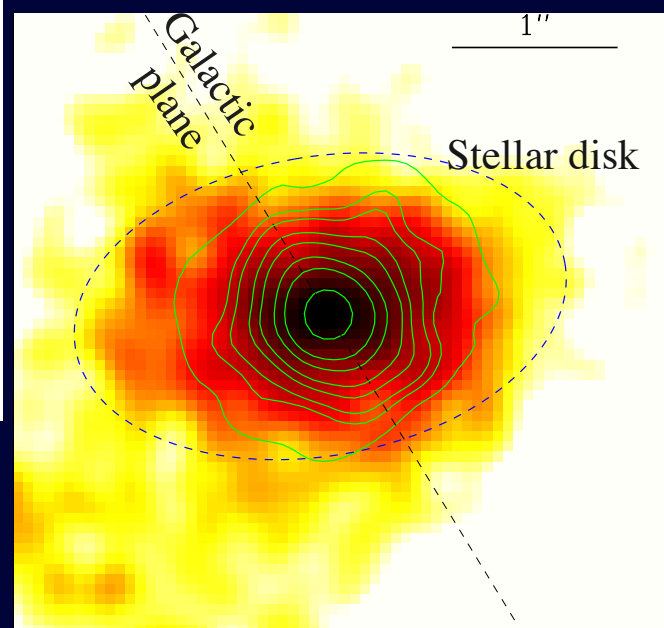
Residual



Key best-fit model parameters

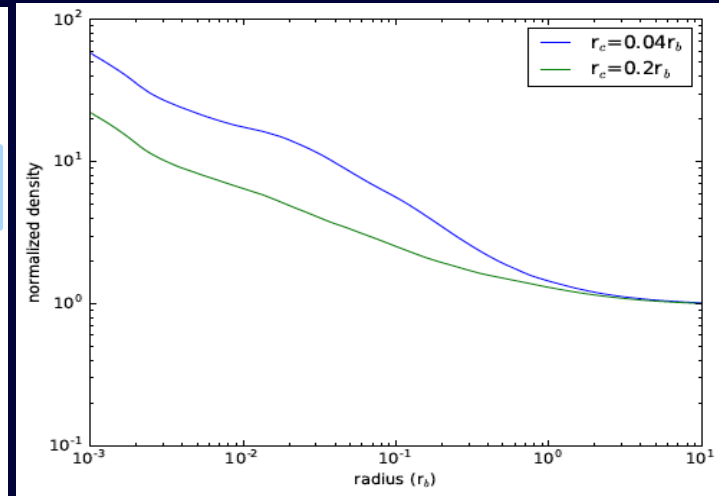
θ_I (deg.)	126.4 (125.0,127.7)
θ_P (deg.)	99.1 (97.8,100.5)
r_c/r_b	0.058 (0.052,0.064)
T_b (K)	$1.30e7$ ($1.24e7, 1.38e7$)
n_b (cm $^{-3}$)	187.0 (174.9,197.6)
α	4.95 (3.96,6.76)
$\log_{10}(N)$	2.69 (2.18,3.63)

Consistency between the orientations of the accretion flow and the stellar disk.



Key best-fit model parameters

θ_I (deg.)	126.4 (125.0,127.7)
θ_P (deg.)	99.1 (97.8,100.5)
r_c/r_b	0.058 (0.052,0.064)
T_b (K)	1.30e7 (1.24e7,1.38e7)
n_b (cm ⁻³)	187.0 (174.9,197.6)
α	4.95 (3.96,6.76)
$\log_{10}(N)$	2.69 (2.18,3.63)

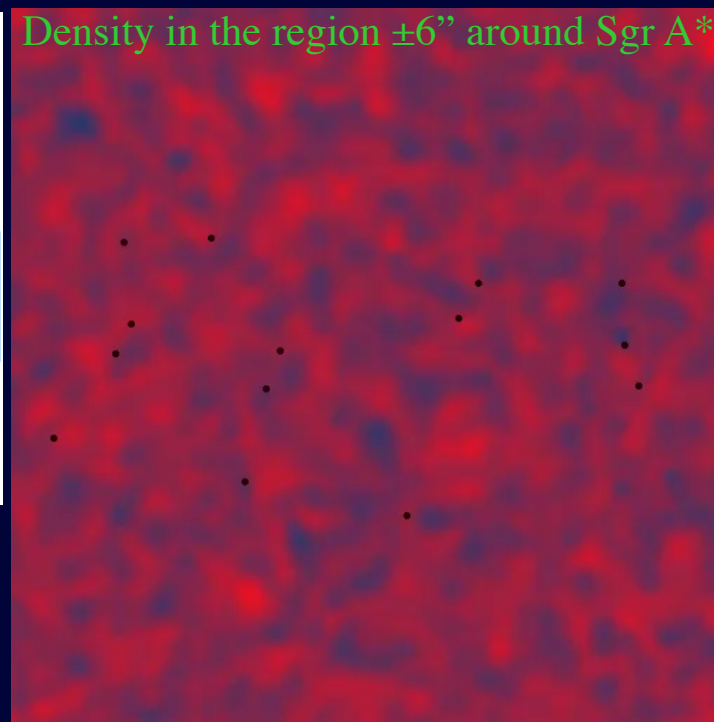


- First direct estimate of the centrifugal radius or **mean angular momentum** of the accretion flow.
- Outflow, **needed for the angular momentum loss**, flattens the radial density profile.

Key best-fit model parameters

θ_I (deg.)	126.4 (125.0,127.7)
θ_P (deg.)	99.1 (97.8,100.5)
r_c/r_b	0.058 (0.052,0.064)
T_b (K)	1.30e7 (1.24e7,1.38e7)
n_b (cm ⁻³)	187.0 (174.9,197.6)
α	4.95 (3.96,6.76)
$\log_{10}(N)$	2.69 (2.18,3.63)

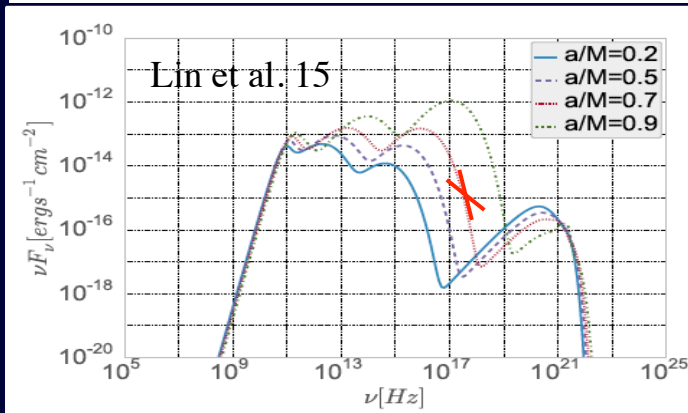
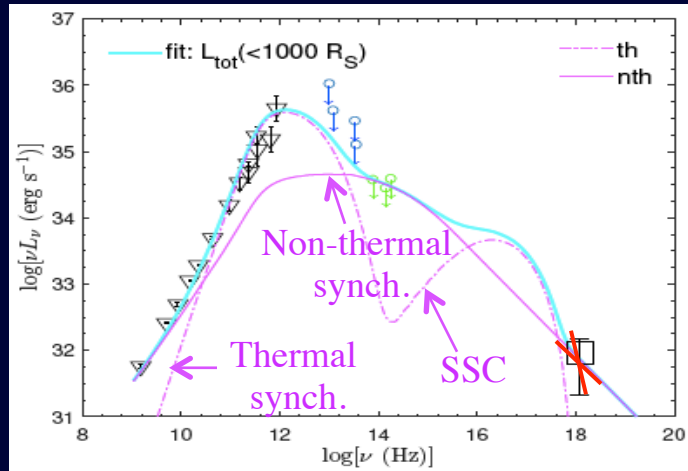
- Consistent with the values expected from the cluster wind.
- Expect significant change of the accretion rate with time



Russell, QDW, & Cuadra 16

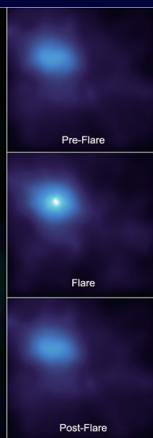
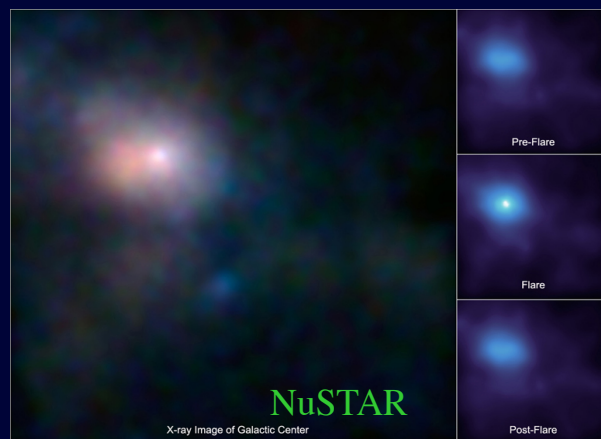
Phenomena and physical processes in the innermost region

Quiescent point-like X-ray emission

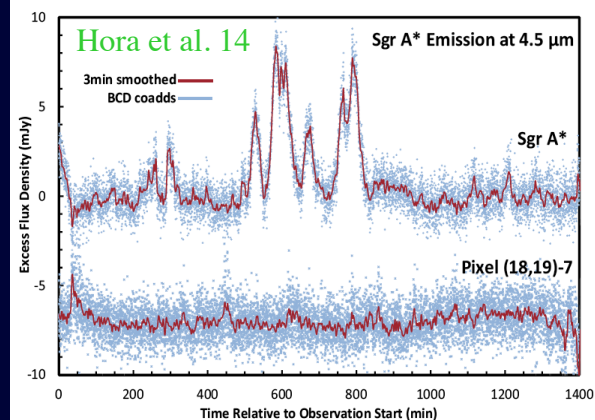


- Emission from $r < \text{a few } \times 10^2 r_s$
-- the simulation inner boundary
- Account for $\sim 4\%$ of the observed counts
- Photon index $\Gamma = 3.5\text{--}7.5$
- Emission mechanisms:
 - ~~Bremsstrahlung~~
 - ~~Synchrotron~~
 - Synchrotron-self-Compton (SSC) + possible synchrotron from nonthermal electrons

X-ray and NIR flares of Sgr A*



Hora et al.



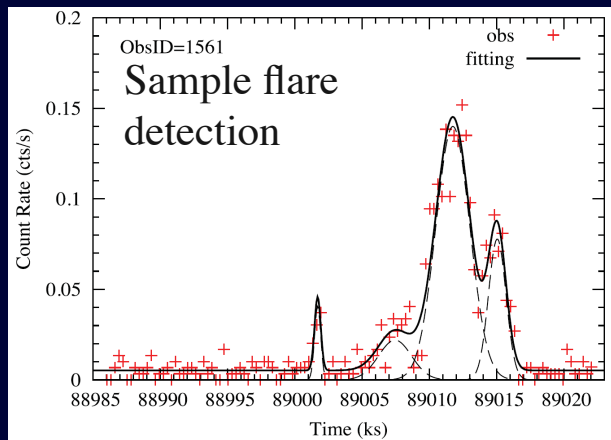
- ~ 100 flares in X-rays
(from Chandra/XMM-Newton/Swift/NuSTAR)
- ~ 2 flares per day
- Duration $\tau \sim 1$ hour
- $L_X \sim 10^{33}\text{-}10^{35}$ erg/s

Baganoff et al. 01; Ponti et al. 15; Yuan & Wang 16;
Zhang et al. 17; Mossoux & Grosso 17

- A few times more frequent in NIR
- Polarized \rightarrow synchrotron
- NIR flare region size $< \sim 1 r_s$
- Every X-ray flare has NIR counterpart, lasting longer, but not vice versa.

Genzel et al. 03; Dodds-Eden et al. 09; Hora et al. 14

X-ray flare detection and statistics

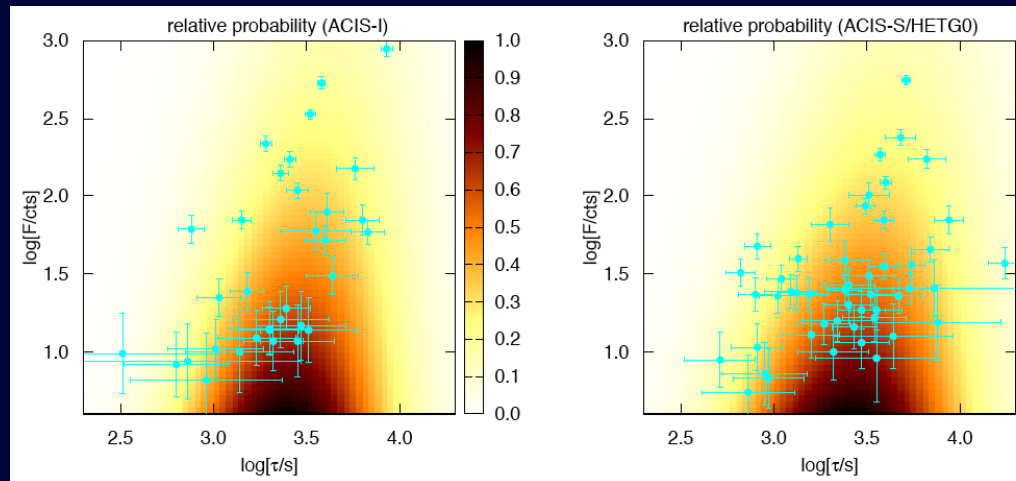


- Maximum likelihood fitting
- Direct pileup correction
- Gaussian decomposition
- Parameter error measurement
- Detection incompleteness/bias correction

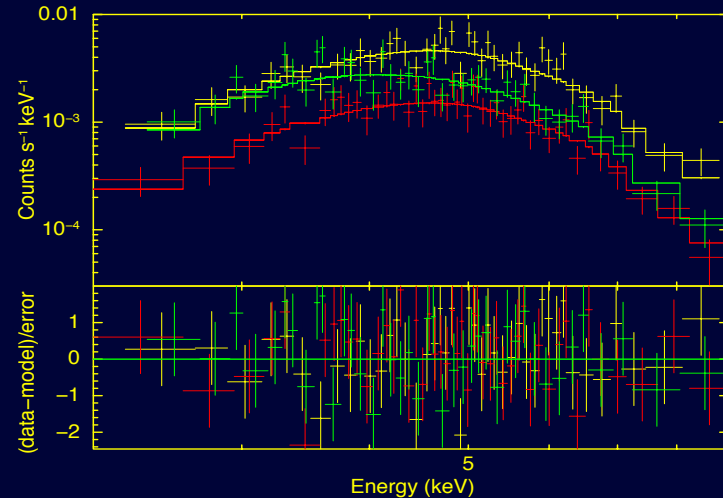
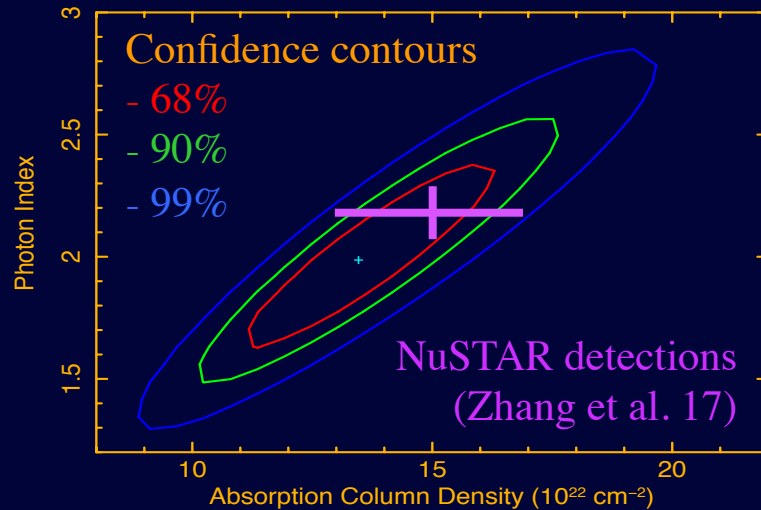
MCMC Bayesian analysis:

- $dN/dF \propto F^{-\alpha}$, $\alpha=1.7\pm0.2$
- $\tau \propto F^{-\beta}$, $\beta=0.09\pm0.16$
- $\sigma(\log \tau) = 0.28\pm0.07$

Yuan & Wang 16; Yuan, QDW et al. 17



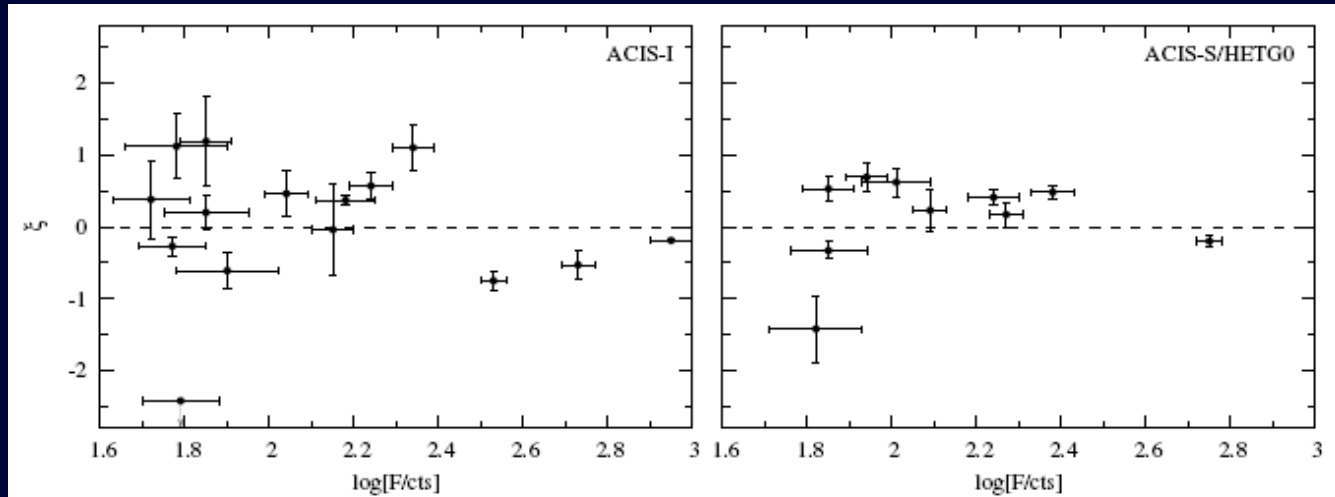
Spectral analysis of X-ray flares



- Power law fit to the accumulated spectra of weak and strong fares
- Consistent single power law from NIR to hard X-ray
- No spectral dependence on flare brightness \rightarrow single origin of the flares

Yuan, QDW et al. 17

Lightcurve asymmetry of X-ray flares

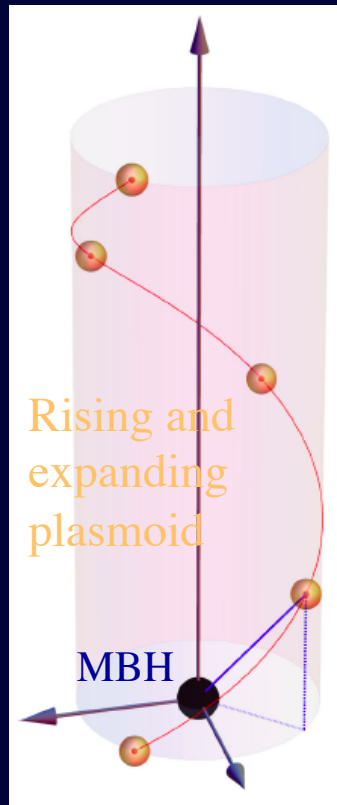


Fitting with the asymmetric Gaussian function for bright flares (# of counts > 50):

- \sim equal chance for $\xi > 0$ and $\xi < 0$
- No spectral difference between the rising and decaying phases

Yuan, QDW et al. 17

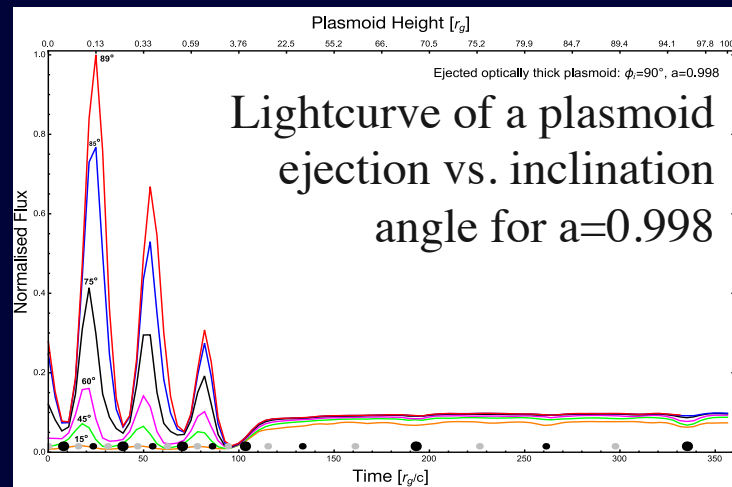
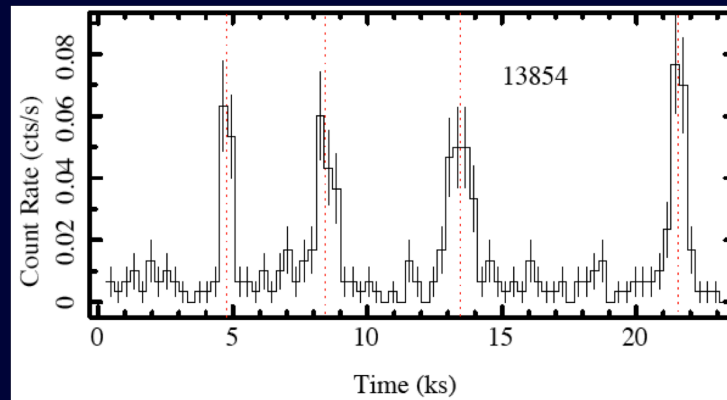
Relativistic effects & clustering properties



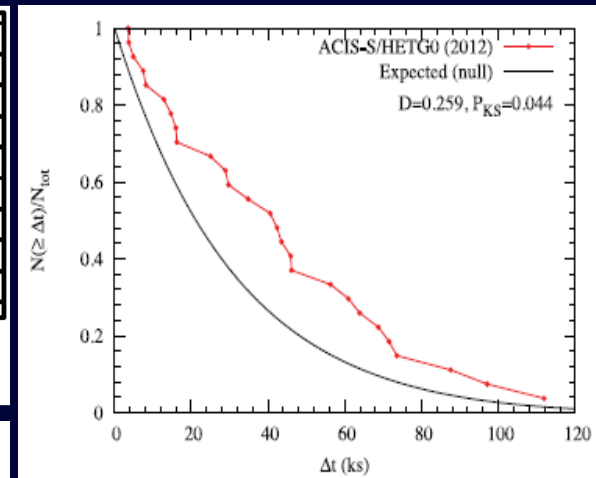
Rising and
expanding
plasmoid

MBH

Younsi & Wu 15



Lightcurve of a plasmoid
ejection vs. inclination
angle for $a=0.998$



Detection of flare
clustering on time
scales of ~ 40 ks
($>95\%$ confidence)

Flare generation mechanisms

Magnetic reconnection



Differential rotation \rightarrow magnetic stress and helicity in flux ropes \rightarrow reach a threshold \rightarrow fast reconnection \rightarrow launch plasmoid and/or particle acceleration

Markoff et al. 01; Dodds-Eden et al. 10; Li et al. 17

Asteroid tidal disruption



Asteroids (sizes >10 km) approach ~ 1 AU of the MBH \rightarrow fragments \rightarrow evaporation by friction; plasma instability \rightarrow heat electrons to $\sim 10^2$ GeV

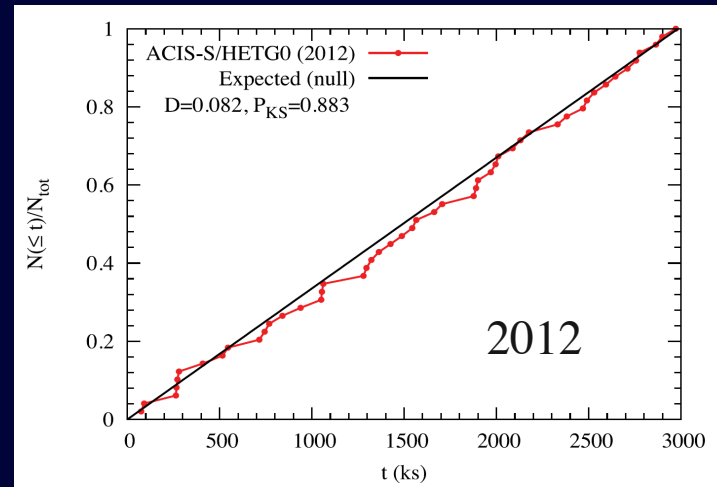
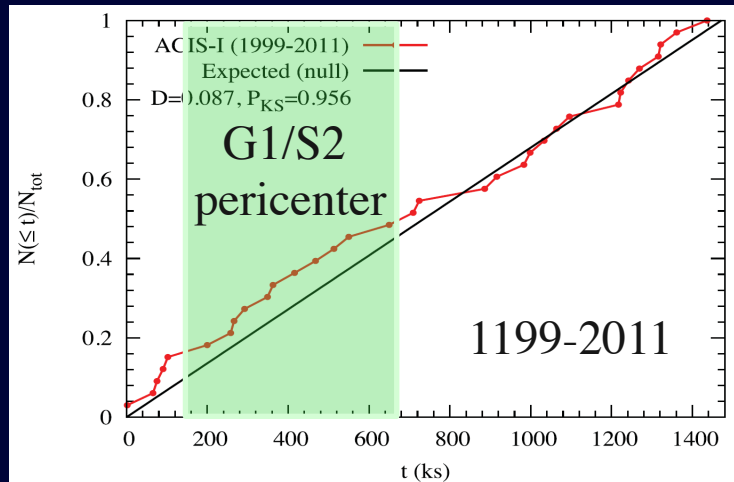
Cadez et al. 08; Kostic et al. 09; Zubovas et al. 12

Preliminary test of the models

	Rate	dN/dF	τ vs. F	Cluster	Shape	Spectrum
Reconnection	✓	×?	×?	✓?	×?	?
Disruption	✓	✓	✓	?	×?	?

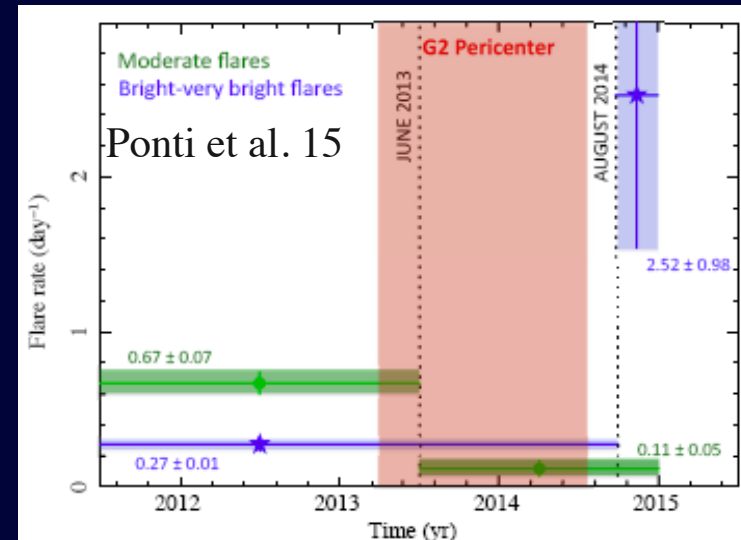
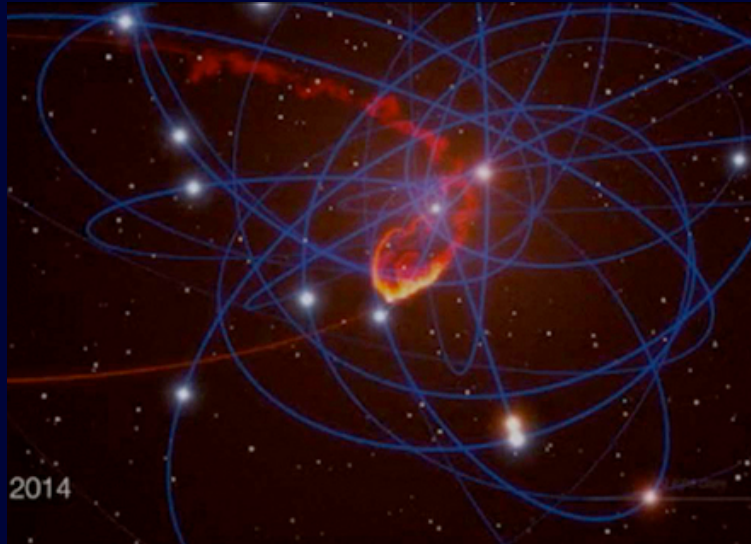
- Magnetic reconnection may be described by the self-organized criticality (SOC) theory (Katz 1986; Bak et al. 1987), which predicts $\alpha \sim 1.5$ and $\beta \sim 0.5$ for spatial dimension $S = 3$.
- Tidal disruption of asteroids from a putative “Super-Oort cloud” around Sgr A* $\rightarrow \alpha \sim 1.7-2$ and $\beta \sim 0$ (Zubovas et al. 12).
- Relativistic effects are likely important for the clustering and shape properties.
- Emission models are yet to be developed for the comparison.

Evolution of quiescent and flare emission



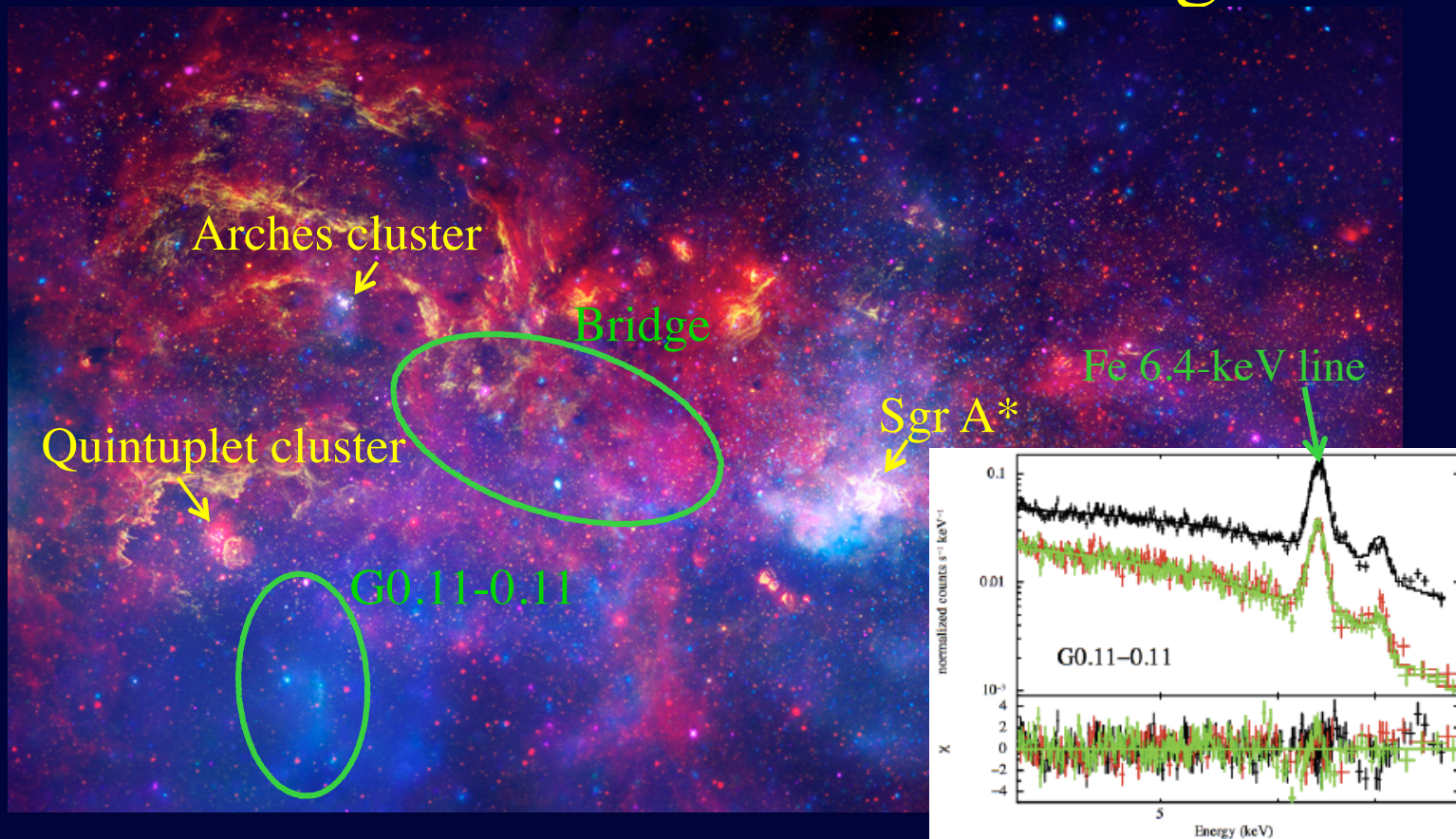
No significant change in the flare rate or quiescent emission from 1999-2012, even around/after G1/S2 passage

Recent G2 passage and X-ray flare rate

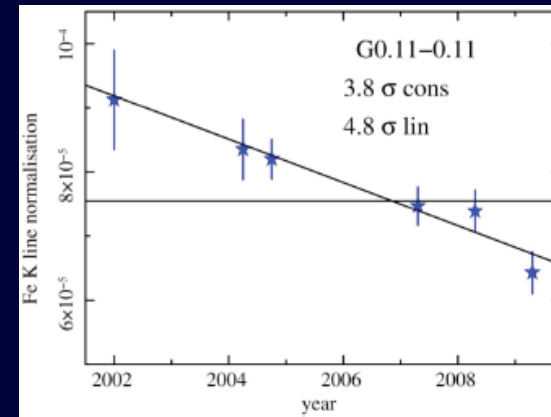
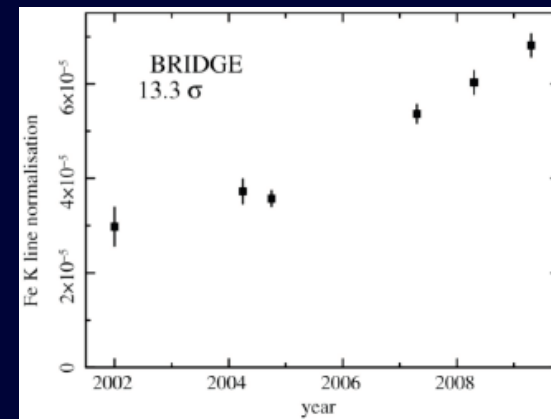
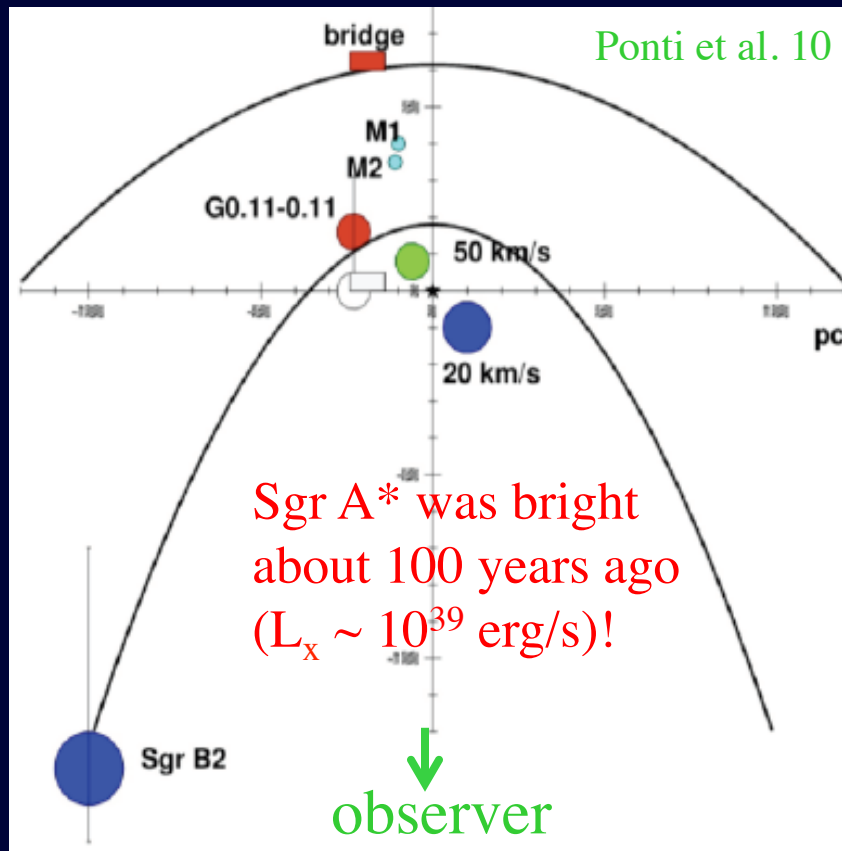


- In Spring 2014, G2 reached the pericenter at $1.5 \times 10^3 r_s$.
- Faint flare rate decreased right before and after the passage (Mossoux & Grosso 17), while bright flare rate increased months later (Ponti et al.15), although their connection to G2 is not clear.

Evidence for recent bursts of Sgr A*



X-ray reverberation of bursts



Life cycle of galactic nuclear activity

Cold gas accretion → SF &
AGN → strong wind →
blows out remaining cold gas
shuts off cold accretion



How energetic is the
AGN outflow?

Accretion from hot plasma
→ RIAF, emission mostly
thermal at large radii, weak
nonthermal near the MBH



How energetic is the
outflow of the RIAF?



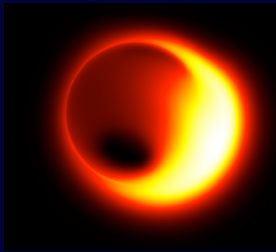
Cycle interrupted by
disruptions of asteroids/
planets/stars + perhaps
dense clouds

When the wind weakens

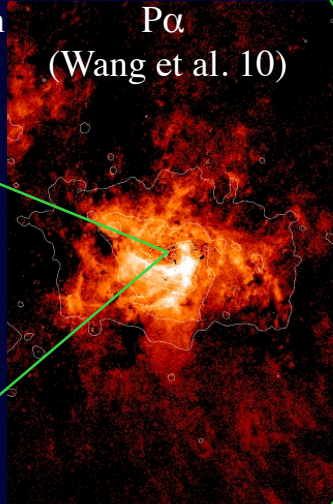
From Sgr A* to Galactic ecosystem

- Better modeling + multi-wavelength observations from radio-X-ray → flare generation and emission mechanisms
- Structures over a 10^{10} scale range → history and energetics of Sgr A* episodes → effects on Galactic ecosystem

MM simulation
(Broderick)



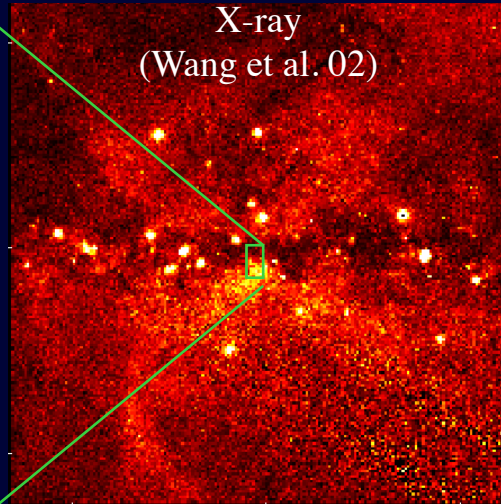
P α
(Wang et al. 10)



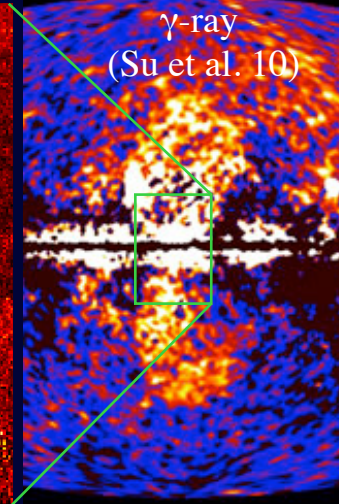
X-ray
(Wang et al. 02)



X-ray
(Wang et al. 02)



γ -ray
(Su et al. 10)



Acknowledgement

Thanks to many collaborators, especially Qiang Yuan (UMass/PMO), Shawn Roberts (UMass), Yan-Fei Jiang (CfA), Jerry Ostriker (Columbia U.), and the Chandra XVP collaboration, as well as NASA for data and funding.

Please come to my contributed talk: “X-ray Imaging and Spectroscopy of the Andromeda Galaxy's Nuclear Feedback”, 10:30AM this Thursday.